**Dual burst wavelet LDA processor implemented and tested on real flows**

by

W.K.Harteveld[(1)], R.F. Mudde[(2)] and H.E.A. Van den Akker

Delft University of Technology

Kramers Laboratorium voor Fysische Technologie

Prins Bernhardlaan 6, 2628 BW Delft; the Netherlands

Tel: +31152787084, Fax +31152782838

[(1)]E-Mail: w.k.harteveld@tnw.tudelft.nl

[(2)]E-Mail: r.f.mudde@tnw.tudelft.nl

## ABSTRACT

The accurate measurement of turbulence spectra up to high frequencies requires data with high accuracy in both the Doppler frequency and the burst arrival time, as well as a short processor delay time, even in the presence of high noise levels which can be encountered in e.g. bubbly flows. Most traditional burst processors have been specifically designed to provide reliable Doppler frequency estimates, but do not provide accurate arrival time estimates, even though an accurate arrival time estimate also can improve the Doppler frequency estimate accuracy. Overlapping bursts are usually rejected, since these may provide unreliable frequency estimates. The rejection leads to an effective processor delay time.

The current paper discusses the application of a processor to LDA data, in particular bubbly flow. The processor employs the combination of the wavelet technique (Van Maanen en Nijenboer (1996)) and algorithms that can process overlapping (dual) bursts (like Nobach (2002)). The use of the wavelet technique, i.e. a model burst is fitted to the data, results in effective noise suppression by optimal weighing of the data. This provides a high accuracy for the Doppler frequency estimate as well as the transit time estimate both for single bursts and dual bursts.

The processor delay time is approximately halved (see Figure 1) by allowing for dual bursts. This is done by separating bursts either in the temporal or spectral domain. The direct use of the (iterative) wavelet technique for dual burst processing is limited by the peak broadening resulting in more difficult burst separation. Therefore, elements of the iterative wavelet technique are combined with separation techniques using the powerspectrum and envelope of the bandpassed signal. Temporal separation is achieved by fitting the envelope with a Gaussian curve, subsequently the secondary burst is suppressed by weighing by a window based on the fit. The spectral separation employs similar envelope fits and suppression, combined with bandpass filtering. The techniques provide good results for both the burst separation and noise suppression. Tests with bubbly flows show that the combination of the software burst detector, processor and validation routines allows increased datarates with similar accuracy if compared with a traditional commercial hardware processor. The halving of the processor delay time is determined from the particle interarrival time distribution. This allows the investigation of turbulence spectra up to higher frequencies.

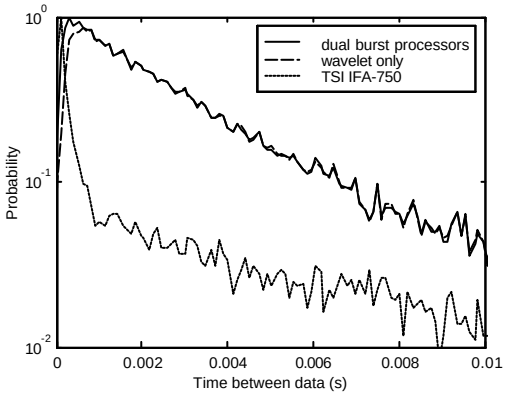


**Figure 1. Particle interarrival time: delay time halved by using dual burst processor.**

## 1. INTRODUCTION

Over the years a lot of attention has been given to the estimation of the frequency of a Doppler signal (an overview can be found in Albrecht et al (2003)). Accurate estimation is an essential step in the processing of the Laser-Doppler Anemometry (LDA), e.g. for estimation of accurate turbulence power spectra. The noise accompanying the Doppler burst leads to an inaccuracy in the velocity estimate. This noise produces a noise floor in turbulence power spectra, obscuring higher frequency information. An accurate Doppler frequency estimate is, however, not the only requirement for the determination of accurate turbulence spectra. For a long time, the lack of accurate estimators was a major limiting factor in the determination of turbulence spectra. More refined estimators (Benedict et al (2000), Broersen et al (2000)) allow the estimation of the spectra at higher frequencies. This, however, puts higher demands on the accuracy of the arrival time. Furthermore, the estimation of higher frequencies requires a high datarate. Most estimation procedures provide unreliable frequency estimates if overlapping bursts are processed (i.e. two or more particles are in the measurement volume at the same time): the location of the peak in the power spectrum is biased. Therefore, these bursts are rejected from the velocity signal. This effectively leads to a processor delay (or dead) time: if the second particle arrives within this time after a previous particle, it is excluded. As a result, the maximum frequency that can be estimated in the turbulence spectrum is limited.

Van Maanen (1999), Nobach and Van Maanen (2001) and Van Maanen and Nijenboer (1996) have previously shown that a very reliable technique to estimate accurately the Doppler frequency and arrival time is by using wavelets, i.e. by fitting a model of the burst to the data. This technique uses the a priori information about the Gaussian burst envelope shape to provide a high accuracy for these estimates. Nobach and Van Maanen (2001) used artificially generated data to show how the noise in the signal is effectively suppressed and that for many cases the accuracy of the Doppler frequency and arrival time approaches the Cramér-Rao lower bound. This technique by itself, however, still assumes the presence of a single burst and does not solve the delay time problem. Nobach (2002) has considered the option to improve the signal validation by allowing for dual-burst signals. A signal processing technique is proposed where three estimators are used. The first estimator assumes a single burst is present and processes it as such. The other processors assume a dual-burst is present. The first dual-burst processor attempts a separation in the time domain after evaluation of the envelope. The second dual-burst processor attempts the separation in the spectral domain. The study pays little attention to the effect of noise in the signal.

The present work considers the combination of the wavelet technique (WT) with the dual-burst approach to a 'dual-burst wavelet processor'. This combination should provide both a short processor delay time, and good performance in the presence of noise: accurate arrival time estimates and Doppler frequency estimates.

The development of the processor is performed especially for use with LDA in bubbly flows, although its use is not limited to this flow type. The application of other measurement techniques to bubbly flows has severe limitations. For instance, PIV is not possible at higher void fractions and larger scale equipment due to the limited optical accessibility. Hot film probes suffer from their intrusive nature and their liquid velocity signals contain contributions from the bubble which need to be identified and removed. LDA does not have these problems as predominantly the seeding velocity is measured. Nevertheless, the use of LDA in bubbly flow also has its complications. The reflections and scattering by the bubbles give a much higher noise level. The higher noise level may lead to multiple validation: bursts corresponding to a single particle appear more than once in the final velocity signal. Bubbles crossing the laser beams create gaps in the data. This results in reduction of the datarate and an increase in the number of long intervals in the particle interarrival time distribution, i.e. the Poisson nature of the interarrival distribution is no longer preserved. The flow in a bubble column is characterized by no net liquid flow. If very uniform gas injection is used the mean axial velocity is low (typically in the range -0.05 m/s to 0.05 m/s) but the fluctuations are much larger (e.g. in the range -0.4 m/s to 0.4 m/s). This may lead to relatively big deviations in the moments due to various bias sources. The application of the dual-burst wavelet processor may help in dealing with the problems created by the high noise levels, low datarate etc. For instance, the seeding density may be further increased. In addition, by storing the entire LDA signals and use flexible processing using software, extra insight can be gained about problems associated with the use of LDA in the bubbly flows.

The present paper describes the implementation of the algorithms for the dual burst wavelet processor. In particular, attention is paid to the combination of the dual-burst approach and wavelet approach. The application of the processor to real data is discussed, in particular for bubbly flow. Most algorithms were developed using test bursts obtained experimentally in these bubbly flows. The paper first discusses the general approach to the burst processing, followed by the algorithms for the processing of single bursts. Next, the processing of dual bursts is discussed, followed by discussion of the algorithms for detection and validation. The experimental setup used for testst and the results obtained are discussed, followed by conclusions.

## 2. DUAL BURST WAVELET PROCESSING

The process of the estimation of burst parameters is composed of a number of steps shown in Figure 2.

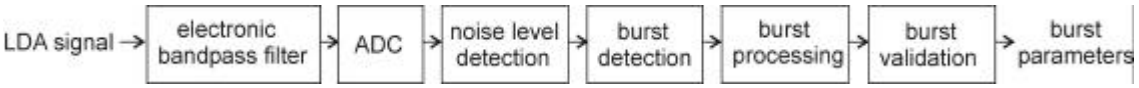


**Figure 2. Procedure of LDA signal processing.**

These will be discussed in more detail in the reset of the paper. First, an electronic bandpass filter is applied which serves as an anti-aliasing filter and removes the pedestal and noise. The LDA signal is sampled continuously at a high frequency resulting in datafiles of multiple GBs. Next, the signal is processed offline via the use of software written in C++. First, the noise level is determined. This is done to allow automatic setting of the detection parameters and processing parameters. Next, the approximate burst locations are determined by the burst detector. The burst processor estimates various parameters of the burst. Finally, a separate validation procedure is performed which removes outliers. The separate validation procedure allows quick study of the effect of validation parameters, without the need of re-running the computationally intensive burst processing algorithms.

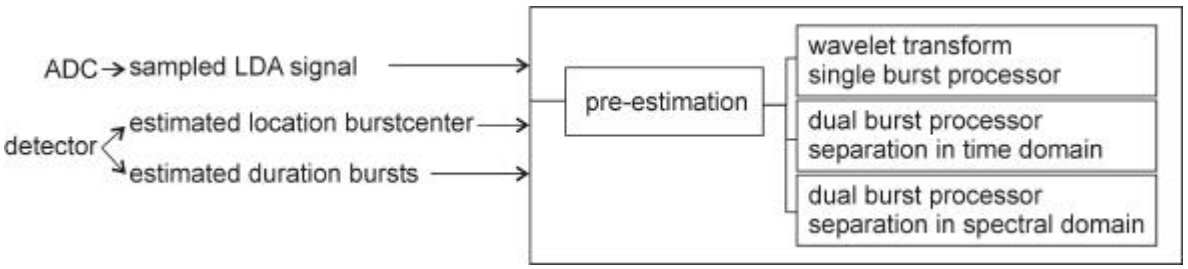


**Figure 3. Burst processing procedure.**

For the dual-burst processing an approach similar to that by Nobach (2002) is taken. For every burst (pair) the parameters are determined in parallel by three processors (see Figure 3). This is done since a priori it is not known whether a single or dual burst is present. The first processor considers the signal fragment as a single burst, the other two processors consider the signal fragment as a dual burst. The decision which estimate should be used is made in the validation step. Since the single burst processor is based on the iterative wavelet transform, a pre-estimation is required for several burst parameters. In the following sections the algorithm components are discussed in more detail.

## 3. SINGLE BURST PROCESSING

The principles of the wavelet transform technique are discussed as well as an explanation for its performance. Subsequently, techniques for the envelope estimation and the pre-estimation are discussed.

### Wavelet transform technique

The processing of single bursts with the wavelet transform technique is considered. For more details, the reader is referred to Van Maanen and Nijenboer (1996), Nobach and Van Maanen (2001) and Van Maanen (1999). A detected burst is passed to the processors. Its signal y(t) is mean-free, has N points and has been sampled with frequency $f_s$ at times $t_i=i\Delta t$ (i= 0 … N-1; $\Delta t=1/f_s$). The wavelet transform tries to fit the following signal model to this burst (arrival time $T_a$, transit time $T_t$, Doppler frequency $f_D$, phase $\phi$ and amplitude A):

$$s(t_i) = Ae^{-\frac{8(t_i-T_a)^2}{T_t^2}}\cos(2\pi f_D t_i + \phi) \tag{1}$$

The Wavelet Transform (WT) in complex notation of y(t) is given by:

$$\begin{aligned} \mathrm{WT}\{y\}(f_D, T_a) &= \sum_{i=0}^{N-1} y(t_i) e^{-\frac{8(t_i-T_a)^2}{T_t^2}} e^{-2\pi j f_D t_i} \\ &= \sum_{i=0}^{N-1} y(t_i) E(t_i; T_a) C(t_i, f_D) \end{aligned} \tag{2}$$

with transform kernels $E(t_i;T_a) = e^{-\frac{8(t_i-T_a)^2}{T_t^2}}$ and $C(t_i, f_D) = e^{-2\pi j f_D t_i}$.

The estimates of the Doppler frequency $\hat{f}_D$ and arrival time $\hat{T}_a$ can be found by maximizing the magnitude of the wavelet coefficient:

$$(\hat{f}_D, \hat{T}_a) = \max(|\mathrm{WT}\{y\}(f_D, T_a)|) \quad (3)$$

The maximization is performed iteratively. A pre-estimation algorithm determines a first estimate of $\hat{f}_D$ and $\hat{T}_t$: $\hat{f}_{Dpre}$ and $\hat{T}_{tpre}$. The estimate for the transit-time is held constant during the following calculations. Next, the algorithm calculates the wavelet coefficients for all discrete arrival times at fixed frequency $\hat{f}_{Dpre}$ and determines the value of the arrival time where their magnitude is maximized:

$$\hat{T}_a = \max\{|\mathrm{WT}\{y\}(\hat{f}_{D,pre}, T_a)|\} \quad (4)$$

Nobach and Van Maanen (2001) showed how the wavelet coefficients can be efficiently calculated for a fixed frequency. With $E_0 = e^{-\frac{8t_i^2}{T_t^2}}$ the coefficients at $T_a = k/f_s$ (k=0 … N-1) are obtained using:

$$\mathrm{DFT}\{\mathrm{WT}\{y\}(f_D, k/f_s)\} = \mathrm{DFT}\{y \cdot C\} \cdot \mathrm{DFT}\{E_0\} \quad (5)$$

The Doppler frequency is found at the location of the maximum:

$$\hat{f}_D = \mathrm{argmax}\{|\mathrm{WT}\{y\}(f_D, \hat{T}_a)|\} \quad (6)$$

The wavelet coefficients can be calculated via the DFT, since:

$$\mathrm{WT}\{y\}(f_D, \hat{T}_a) = \mathrm{DFT}\{y \cdot E(t_i, \hat{T}_a)\} \quad (7)$$

The estimate $\hat{f}_D$ is obtained from the coefficients using a three-point Gaussian interpolation algorithm. The phase estimate $\hat{f}$ is required for validation purposes. It is estimated from the FFT of the signal using the method described in Nobach and Van Maanen (2001). The same authors showed that one frequency iteration and one arrival time estimate are sufficient. This is due to the symmetry of the Gaussian peak in the two-dimensional ($f_D$, $T_a$) domain. Consequently, we obtain the algorithm shown in Figure 4.

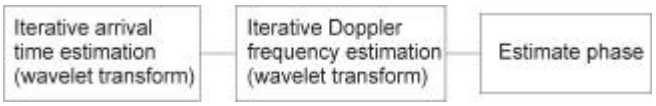


**Figure 4. Wavelet Transform single burst processor**

The wavelet transform provides improved accuracy in the Doppler frequency and arrival time estimates by optimal weighing of the signal. If for instance the Doppler frequency is determined, the effective windowing operation of the wavelet transform provides the optimal peak-to-noise level ratio in the wavelet coefficients, better than can be achieved with traditional DFT-techniques. A priori knowledge about the peak shape can give further increase in accuracy via peak fitting. The wavelet transform preserves the Gaussian peak shape, which is not the case for DFT techniques with other window shapes or clipping.

**Pre-estimation**

The iterative wavelet transform requires a pre-estimate for the transit time and the Doppler frequency. This is provided by the pre-estimation algorithms (Figure 5). These also provide parameters for validation afterwards, such as the amplitude.


**Figure 5. Pre-estimation procedure**

The Doppler frequency is determined from the peak in the power spectrum. A common technique for improving the accuracy is spectral peak interpolation, such as peak fitting (Matovic and Tropea (1991)). The peak in the powerspectrum of a Gaussian burst has again a Gaussian shape. From a Gaussian fit to the spectral peak not only the Doppler frequency, but also the transit time can be estimated. The power spectrum peak is fitted over a variable number of points by minimizing the weighted least squares criterion

$$L(\hat{T}_{tpre1}, \hat{f}_{D,pre1}, \hat{K}) = \sum_{i=i_1}^{i_2} \frac{(\ln(|DFT\{y_1\}(f_i)|^2) + \frac{p^2 \hat{T}_{t,pre1}^2}{4}(f_D - \hat{f}_{D,pre})^2 - \hat{K})^2}{s^2_{\ln(|DFT\{y_1\}(f_i)|^2)}} \quad (8)$$

with respect to the estimates $\hat{K}$, $\hat{T}_{t,pre1}$ and $\hat{f}_{Dpre}$. The fit requires information about the accuracy of $\ln(|\mathrm{DFT}\{y_1\}(f_i)|^2)$, which has been investigated via a semi-empirical analysis of artificial bursts. This shows that if a signal $y_1(t)$ is composed of a noiseless burst $s_1(t)$ and random noise $n_1(t)$ ($y_1(t)=s_1(t)+n_1(t)$), the variance of $\ln(|\mathrm{DFT}\{y_1\}(f_i)|^2)$ is approximately given by:

$$s^{2}_{\ln(|DFT\{y_1\}(f_i)|^2)} \approx 2.21\frac{\text{mean}(|\text{DFT}\{n_1\}(f)|^2)}{|\text{DFT}\{s_1\}(f_i)|^2} \tag{9}$$

for $\frac{\text{mean}(|\text{DFT}\{n_1\}(f)|^2)}{|\text{DFT}\{s_1\}(f_i)|^2}$<0.4. However, since $|\text{DFT}\{s_1\}(f_i)|^2$ is not known, $|\text{DFT}\{y_1\}(f_i)|^2$ is used. This leads in general to underestimation of $s^{2}_{\ln(|DFT\{y_1\}(f_i)|^2)}$, especially for the weaker parts of the burst peak. The underestimation of $s^{2}_{\ln(|DFT\{y_1\}(f_i)|^2)}$ in the part of the burst where $|\text{DFT}\{y_1\}(f_i)|^2$ approaches $|\text{DFT}\{n_1\}(f)|^2$, can lead to erroneous fits, usually resulting in an underestimation of $\hat{T}_{t,pre1}$. Therefore a fit region $i_1$=i=$i_2$ is chosen where $|\text{DFT}\{y_1\}(f_i)|^2 > C_{peak}|\text{DFT}\{n_1\}(f)|^2$. $C_{peak}$ was chosen after tests with real bursts. Tests with artificial bursts show that the technique is fast and gives much higher accuracy and smaller bias for $\hat{f}_{Dpre}$ and $\hat{T}_{t,pre1}$ than traditional three point Gaussian fits. Typical improvements for the standard deviation of the Doppler frequency and transit time estimates are a factor 5 and 10 respectively.

If the bursts are not exactly Gaussian, the transit time estimate can be biased. In addition the noise may cause underestimation. For these reasons the transit time is also determined from the envelope. The envelope is not only required for the transit time estimation, but is also required for the dual burst processors (e.g. arrival time estimation). The envelope of the signal y(t) is obtained with the use of the Hilbert Transform (HT) (Nobach (2001)):

$$\text{ENV}\{y(t)\} = \left|\text{IDFT}\{\text{HT}^{+}\{\text{DFT}\{y(t)\}\}\}\right| \tag{10}$$

where DFT is the discrete Fourier Transform, IDFT its inverse and

$$\text{HT}^{+}\{x\}_i = \begin{cases} x_i & \text{for } i \in (0;N/2) \\ 2x_i & \text{for } 0<i<N/2 \\ 0 & \text{for } N/2<i \le N-1 \end{cases} \tag{11}$$

A low-pass filter can be applied to the envelope to remove oscillations caused by noise. It is important to consider the effect of noise on the envelope estimate, however. Figure 6 (obtained with an artificial burst with $A_1$=4 and $\sigma^2_{n1}$=1) illustrates that:

$$\text{ENV}\{s(t)+n(t)\} < \text{ENV}\{s(t)\}+\text{ENV}\{n(t)\} \tag{12}$$

Therefore, for accurate estimation of the amplitude, transit time and arrival time of bursts, it is important to apply a bandpass filter to the signal before determining the envelope. This bandpass filter should only pass the frequencies where the signal power is larger than the noise power. The envelope of this bandpassed signal is shown in Figure 6, its shape is close to the true envelope.

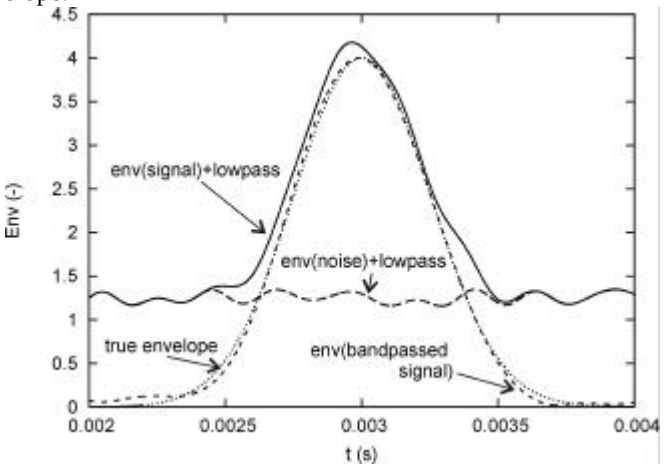


**Figure 6. Comparison of various envelope estimates.**

Similar to Nobach (2001), the transit time can be estimated from the envelope of the bandpass filtered signal:

$$\hat{T}_{tpre2} = \sqrt{\frac{8}{p}}\frac{\sum_{i=0}^{N-1}\text{ENV}\{y_1\}(t_i)}{f_s \max(\text{ENV}\{y_1\}(t_i))} \tag{13}$$

The presence of some reminiscent noise will in general lead to an overestimation. Since the estimate based on the spectral peak can suffer from underestimation, and with lack of further information the average is taken as the final estimate:

$$\hat{T}_{tpre} = \frac{\hat{T}_{tpre1}+\hat{T}_{tpre2}}{2} \tag{14}$$

The amplitude of the burst $\hat{A}_1$ is estimated from the bandpassed envelope:

$$\hat{A}_1 = \max(\mathrm{ENV}\{y_1\}(t_i)) \tag{15}$$

## 4. DUAL BURSTS PROCESSING

In the dual burst processors, the following signal model is fitted to the data:

$$s(t_i) = A_1 e^{-\frac{8(t_i - T_{a1})^2}{T_{t1}^2}} \cos(2\pi f_{D1} t_i + f_1) + A_2 e^{-\frac{8(t_i - T_{a2})^2}{T_{t2}^2}} \cos(2\pi f_{D2} t_i + f_2) \tag{16}$$

### Wavelet transform applied to dual bursts

Doppler frequencies may be estimated by fitting the peak of the coefficients obtained via the DFT or the WT. Similarly, the arrival time may be estimated via a fit of the peak obtained with the wavelet transform or the peak in the estimate of the envelope of the burst. The shapes of the peaks obtained with these techniques differ, however. The shapes of the peak obtained with the |WT| and the $|\mathrm{DFT}|^2$ are given by:

$$|\mathrm{WT}\{s_1\}(f_D, T_a)| \propto A_1 T_{t1} e^{-4\frac{(T_a - T_{a1})^2}{T_{t1}^2}} e^{-\frac{\pi^2 T_{t1}}{16}(f_{D1} - f_k)^2} \tag{17}$$

$$|\mathrm{DFT}\{s_1\}(f_k)|^2 = \frac{\pi A_1^2 T_{t1}^2 f_s^2}{32} e^{-\frac{T_{t1}^2 \pi^2}{4}(f_{D1} - f_k)^2} \tag{18}$$

Comparison of equations (17) (squared) and (18) shows that the use of the WT results in a spectral peak width that is a factor $\sqrt{2}$ bigger than the spectral peak width obtained with the DFT. Similarly, comparison of equations (17) and (16) shows that the temporal width of $|\mathrm{WT}\{s\}(f_D, T_a)|$ is also a factor $\sqrt{2}$ bigger than the width of the burst envelope. The increase of the widths may lead to problems if a dual burst is measured where both bursts have almost the same Doppler frequency and arrival time. Whereas a minor peak overlap may be obtained with the DFT or envelope based estimation techniques, a bigger peak overlap is obtained using the WT technique. This is illustrated in Figure 7 for two artificial bursts with equal frequency and a small arrival time difference. An initial minor temporal overlap in the envelope becomes a severe overlap in the wavelet coefficients. The increased overlap can create a larger bias for the estimate of the Doppler frequency and arrival time. For even larger overlaps it may even make the detection of the second peak impossible. Therefore, direct use of the wavelet transform for the estimation of dual bursts is not suitable and an alternative approach is taken incorporating only elements of the wavelet transform.

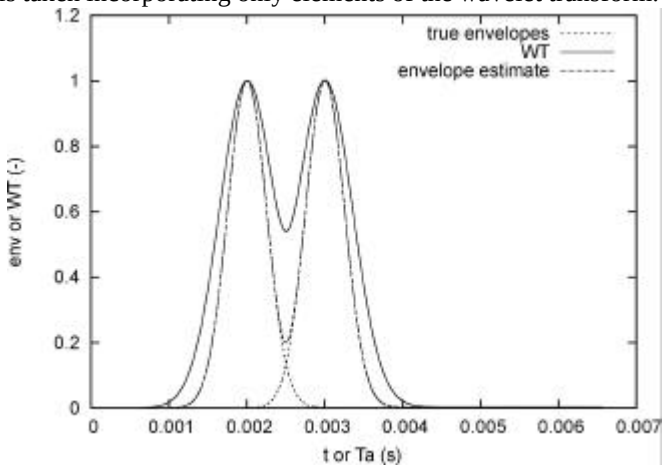


**Figure 7. Comparison envelopes and wavelet coefficients for a dual burst.**

Tests with artificial bursts show that the variance of the arrival time estimate using the envelope of the bandpassed signal is only slightly bigger than the variance using the wavelet transform. Therefore, the dual burst processor with temporal separation uses this envelope to estimate the arrival time instead of the wavelet transform. For the dual burst processor employing spectral separation, drift and detectability of the Doppler frequency may also improve by using the original power spectrum instead of the frequency iteration of the wavelet transform. However, this advantage is only present for bursts with very strong temporal overlap (i.e. two particles at almost exactly the same time in the measurement volume) and Doppler frequencies which are very close. These bursts provide little additional information anyway. Therefore, the Doppler frequency is estimated using the frequency iteration of the wavelet transform where maximum noise suppression is obtained. For bursts with strong overlap in time and frequency, further improvements may be obtained by incorporating a third dual-burst processor which uses window shapes which suppress noise effectively, try to suppress the peak by the other burst, but have a smaller widening effect on the peak shape. This is not performed in the current investigation, however.

**Dual burst processor with separation in time**

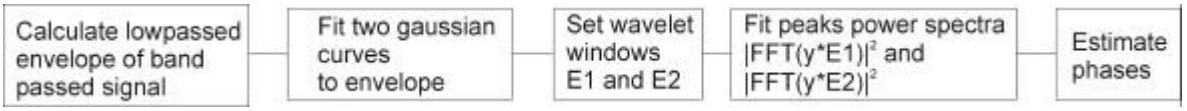


**Figure 8. Dual burst processor with separation in time.**

Bursts with overlap in the spectral domain may be separated if their overlap in time is small. The basic idea is to cut the signal at the point of overlap and process the two parts separately, similar to Nobach (2002). The current processor, however, employs a multiplication by a wavelet window to suppress the other burst and noise. Some measures are implemented to allow for some temporal overlap. Figure 8 shows the algorithm schematically.

First, the signal y(t) (an example is given in Figure 9a) is filtered with a bandpass filter. The pass regions of the filter are based on the amplitude in the power spectrum. This requires an estimate of the noise level and the peak height. Therefore, the biggest peak in the power spectrum P(f) is located (location $f_{max}$, height $P_p$). Adjacent minima with locations $f_{min,s}$ and $f_{min,e}$ are located. The region $f_{ps}..f_{pe}$ around the biggest peak is identified: this is the largest combination of $f_{min,s}..f_{min,e}$ and $f_{max}-f_{width}/2..\ f_{max}+f_{width}/2$, where $f_{width}$ is a spectral peak width based on a burst duration timescale obtained from the noise detector. The noise level $P_n$ is the average power spectrum level outside region $f_{ps}..f_{pe}$.

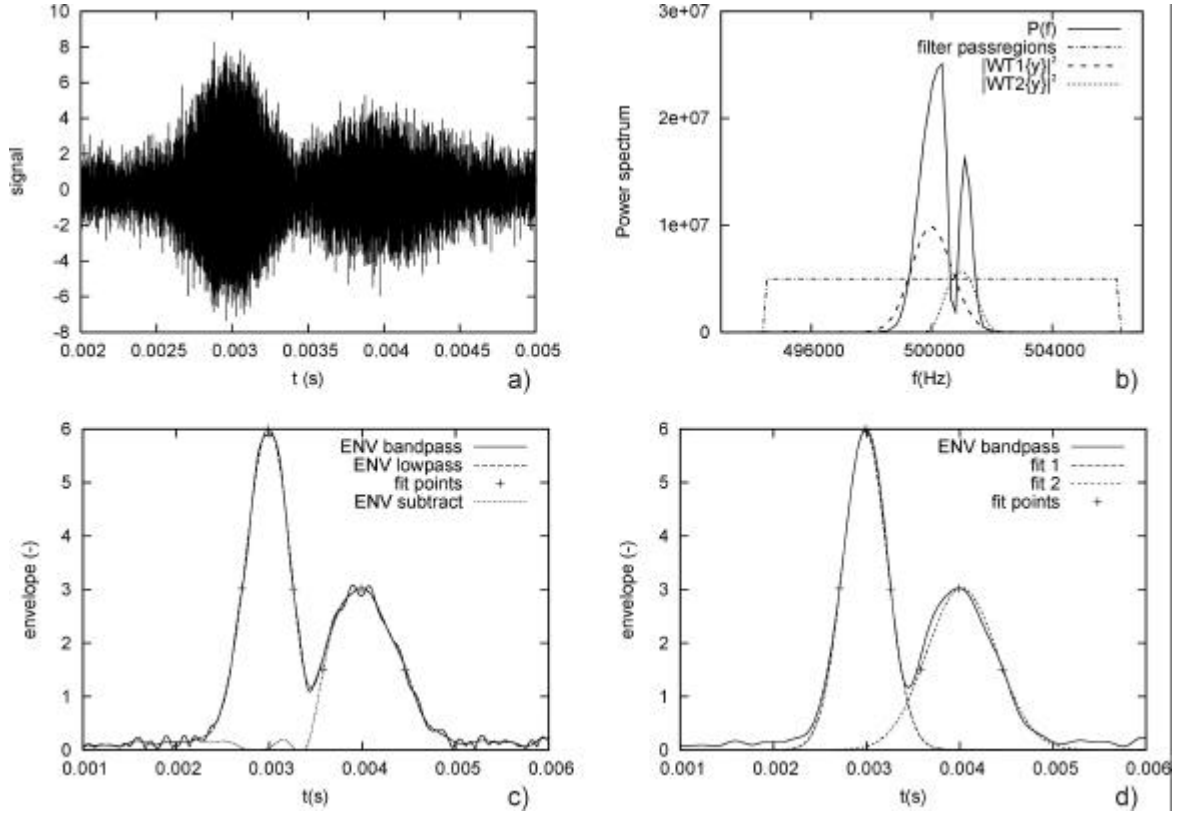


**Figure 9. Steps in dual burst processing with temporal separation. a) Signal b) Powerspectra c) Envelopes d) Fits of envelopes**

The threshold level $P_{threshold}=0.2(P_p-P_n)+P_n$ is set. All frequencies in the power spectrum P(f) with $P(f)>P_{threshold}$ are identified as well as their adjacent frequencies up to the next minima in the power spectrum (Figure 9b). The bandpass filter is set to pass all of these frequencies, and gives filtered signal $y_f(t)$. Next, the envelope $ENV_{bandpass}$ of the bandpass filtered signal is determined using the Hilbert transform. A lowpass filter is used to remove the remaining oscillations from the envelope, providing $ENV_{lowpass}$. Its cutoff frequency is based on the timescale mentioned before. Examples of the envelopes are shown in Figure 9 (c).

Next, the biggest peak in the envelope is identified. A Gaussian curve $G_1^{DT}(t) = \hat{A}_1^{DT} e^{-\frac{8(t-\hat{T}_{a1}^{DT})^2}{(\hat{T}_{t1}^{DT})^2}}$ is fitted to three points to determine the estimates for amplitude $\hat{A}_1^{DT}$, arrival time $\hat{T}_{a1}^{DT}$ and transit time $\hat{T}_{t1}^{DT}$ of the biggest burst. The three points used in the fit are the maximum, and the points at the flanks where the threshold level $\min(ENV_{lowpass})+0.5(\max(ENV_{lowpass})-\min(ENV_{lowpass}))$ is crossed. This is followed by the removal of the biggest burst from the envelope via:

$$\mathrm{ENV}_{subtract}(t) = \max(\mathrm{ENV}_{lowpass}(t) - G_1^{DT}(t), 0) \tag{19}$$

The amplitude $\hat{A}_2^{DT}$, arrival time $\hat{T}_{a2}^{DT}$ and transit time $\hat{T}_{t2}^{DT}$ of the second burst are estimated in the same way, via fitting $G_2^{DT}(t) = \hat{A}_2^{DT} e^{-\frac{8(t-\hat{T}_{a2}^{DT})^2}{(\hat{T}_{t2}^{DT})^2}}$ to three points of $\mathrm{ENV}_{\mathrm{subtract}}$. The fitting procedure is illustrated in Figure 9 c) and d). The Doppler frequencies are estimated with the use of the frequency iteration step of the wavelet transform. The influence of a possible temporal overlap on the peak of the wavelet coefficients is investigated. The noisy signal y(t) is assumed to be composed of two bursts having noiseless signal $s_1(t)$ and $s_2(t)$. If a window with transit time $T_{tx}$ is used, we get (with $\eta_i = 8/T_{t,i}^2$ and $\eta_x = 8/T_{t,x}^2$):

$$|WT\{s_i\}(f_D, T_a)| = \frac{\sqrt{p}\, A_i f_s}{2\sqrt{h_i + h_x}} e^{-\frac{p^2}{h_i + h_x}(f_{Di} - f_D)^2} e^{-\frac{h_i h_x}{h_i + h_x}(T_{ai} - T_a)^2} \tag{20}$$

The peak associated with burst j is estimated using a window with $T_a = T_{a,j}$ and $T_{tx} = T_{tj}$. The wavelet coefficients will contain peaks due to both bursts. The ratio of the amplitudes of the peaks corresponding to burst i and burst j is given by:

$$OC_{ij} = \frac{|WT\{s_i\}(f_{Di}, T_{aj})|}{|WT\{s_j\}(f_{Dj}, T_{aj})|} = \frac{A_i}{A_j}\sqrt{\frac{2h_j}{h_i + h_j}} e^{-\frac{h_i h_j}{h_i + h_j}(T_{ai} - T_{aj})^2} \tag{21}$$

If $OC_{ij} > 0.5$ the overlap is too big, and the window is made more narrow to reduce the influence of overlap. With:

$$\hat{T}_{tj}^{DT*} = \max(2|\hat{T}_{aj}^{DT} - \hat{T}_{ai}^{DT}| - \hat{T}_{ti}^{DT}, \frac{\hat{T}_{tj}^{DT}}{10}) \tag{22}$$

If $OC_{ij} < 0.5$ the standard wavelet transform Doppler frequency iteration method is used for burst j: the overlap is small enough to ensure detection of the correct peak. This gives $\hat{T}_{tj}^{DT*} = \hat{T}_{tj}^{DT}$.

The following window is obtained (for simplicity, we assume that $\hat{T}_{aj} < \hat{T}_{ai}$):

$$E_j^{DT}(t_i; \hat{T}_{aj}^{DT}) = \begin{cases} e^{-\frac{8(t_i - \hat{T}_{aj}^{DT})^2}{(\hat{T}_{tj}^{DT})^2}} & \text{for } t_i \le \hat{T}_{aj}^{DT} \\ e^{-\frac{8(t_i - \hat{T}_{aj}^{DT})^2}{(\hat{T}_{tj}^{DT*})^2}} & \text{for } t_i > \hat{T}_{aj}^{DT} \end{cases} \tag{23}$$

The Doppler frequency of burst j $\hat{f}_{D,j}^{DT}$ is determined using a Gaussian three-point fit of the maximum of $|\mathrm{WT}^{\mathrm{DT}}{}_j\{y\}|^2$, which is determined with:

$$\mathrm{WT}_j^{\mathrm{DT}}\{y\}(f_D, \hat{T}_{aj}^{DT}) = \mathrm{DFT}\{y \cdot E_j^{DT}(t_i, \hat{T}_{aj}^{DT})\} \tag{24}$$

**Dual burst processor with spectral separation**

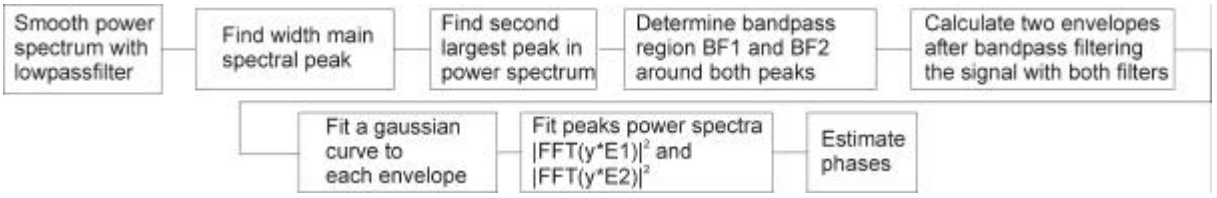


**Figure 10. Dual burst processor with spectral separation**

The dual burst processor tries to perform the separation in the frequency domain by finding the peaks in the powerspectrum due to both bursts and selectively process these using digital filtering. This is again similar to Nobach (2001) but using wavelet techniques and other measures to reduce the influence of noise. A schematic overview of the method is shown in Figure 10.

First, the power spectrum is smoothed since it contains many oscillations. For this purpose a Gaussian lowpassfilter is used. The transit time estimate of the largest-amplitude burst with temporal separation $\hat{T}_{t1}^{DT}$ is used to set the minimum frequency scale $f_w = 4\sqrt{2}/(\pi \hat{T}_{t1}^{DT})$ that should be passed. The filter has transfer function $e^{-i^2/N_c^2}$ with $N_c = f_{p,max}/(2f_w)$, where $f_{p,max}$ is the maximum frequency in the power spectrum. After searching the largest-amplitude power spectrum peak (located at $f_{max1}$), the second largest peak (located at $f_{max2}$) has to be found in the power spectrum. For this purpose, the algorithm determines the frequency range $f_{ps1}..f_{pe1}$ of the main peak that should be excluded from the search. Minima adjacent to the maximum are located: $f_{min1,s}$ and $f_{min1,e}$. The region $f_{ps1}..f_{pe1}$ is the largest combination of $f_{min1,s}..f_{min1,e}$ and $f_{max1}-0.7f_w..\ f_{max1}+0.7f_w$. The bandpass filter frequency ranges are set: for peak *j* the bandpass filter $\mathrm{BF}^{\mathrm{DF}}{}_j$ has frequency pass range $f_{bpsj}..f_{bpej}$. The range is determined in the same way as the search exclusion zone discussed before. For peak *j* the minima adjacent to the peak are determined: $f_{min\,j,s}$ and $f_{minj,e}$. If the peaks are not close

(i.e. $|f_{max1}-f_{max2}|/f_w>2$) the peak width $f_{w\,j,s}$.. $f_{w\,j,e}$ is estimated from the timescale with: $f_{w\,j,s}= f_{max,j}-0.75f_w$ and $f_{w\,j,e}= f_{max,j}+0.75f_w$. Otherwise, $f_{w\,j,s}= f_{max,j}-0.5f_w$ and $f_{w\,j,e}= f_{max,j}+0.5f_w$. Finally, $f_{bpsj}=\min(f_{min\,j,s}, f_{w\,j,s})$ and $f_{bpej}=\min(f_{min\,j,e}, f_{w\,j,e})$. Figure 11 (b) illustrates the procedure.
For each peak, the signal is bandpass filtered and the envelope is determined:

$$\mathrm{ENV}_j^{DF}(t) = \mathrm{ENV}(\mathrm{BP}_j^{\mathrm{DF}}(y(t))) \tag{25}$$

Next, each envelope $\mathrm{ENV}_j^{\mathrm{DF}}(t)$ is fitted with a gaussian curve $G_j^{\mathrm{DF}}(t)$ (Figure 11 c), from which the estimates for amplitude $\hat{A}_j^{DF}$, arrival time $\hat{T}_{aj}^{DF}$ and transit time $\hat{T}_{tj}^{DF}$. The fitting procedure is identical to that for the dual burst processor with temporal separation. Subsequently, the Doppler frequencies are estimated with the use of the frequency iteration step of the wavelet transform. With $E_j^{DF}(t_i;\hat{T}_a) = e^{-\frac{8(t_i-\hat{T}_{aj}^{DF})^2}{\hat{T}_{tj}^2}}$:

$$\mathrm{WT}_j^{\mathrm{DF}}\{y\}(f_D,\hat{T}_{aj}^{DF}) = \mathrm{DFT}\{y\cdot E_j^{DF}(t_i,\hat{T}_{aj}^{DF})\} \tag{26}$$

The Doppler frequency of burst j $\hat{f}_{D,j}^{DF}$ is determined using a Gaussian three-point fit of $|\mathrm{WT}^{\mathrm{DF}}{}_j\{y\}|^2$ of the maximum located in the range $f_{bpsi}..f_{bpei}$.

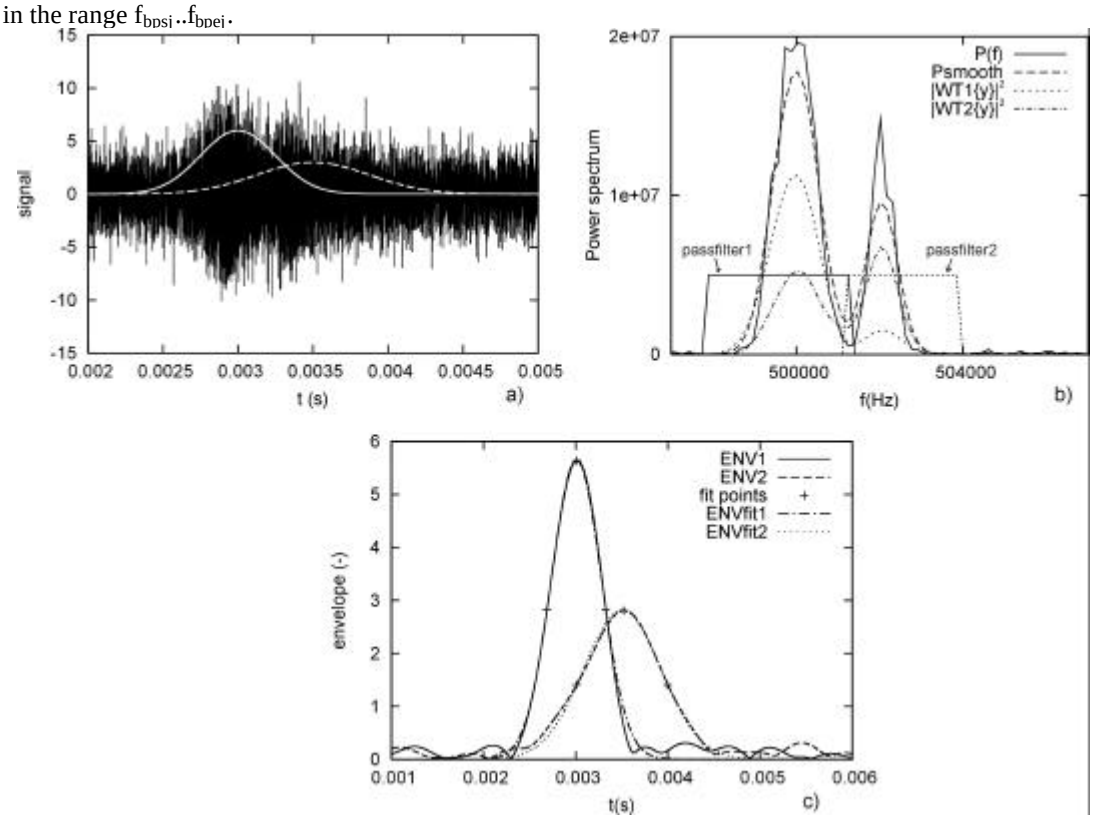


**Figure 11. Steps in dual burst processing with spectral separation. a) Signal b) Powerspectrum, raw and smoothed with bandpass filter ranges and $|\mathrm{WT}|^2$ for both bursts c) Envelope fits.**

## 5. DETECTION AND VALIDATION

### Noise level detection and burst detection

Due to space constraints the noise level detection and burst detection are discussed only briefly. An estimate of the noise level of the LDA signal is required for automatic setting of threshold levels in the burst detector as well as for the burst processing. A rough estimate for this noise level is found by calculating the standard deviation after removal of the bursts from the signal. The bursts are removed by an iterative algorithm based on the pdf of a small part of the signal. If a large fraction of the points differ significantly from the mean, the part of the signal is considered to be part of a burst.
The burst detector is based on an autocorrelation technique, which has similarities with the algorithm by Jenson (1992). The detector should detect bursts with frequencies inside a given range. Delays are selected that correspond to the location of the first maximum of the autocorrelation of signals with these frequencies. A small window is shifted over the signal. The autocorrelation coefficients for these delays are calculated for this window. The maximum autocorrelation coefficient is selected: $A_{acf}(t)$. Burst candidates are found by locating the parts of the signal where $A_{acf}(t)$ exceeds threshold level $A_{acf,threshold}$. False detection is reduced by rejecting burst candidates with duration shorter than a certain threshold, as well as candidates with a mean $A_{acf}(t)$ level lower than a certain threshold. Thresholds are

set automatically, based amongst others on the burst duration and the noise level, to minimize the occurrence of multiple validation, false detection and bias in the burst duration. In addition, the algorithm and sampling rate are optimized to prevent a Doppler frequency dependent probability of detection. At this moment, the settings of the detector are set sensitive to avoid possible bias. This results, however, in a somewhat higher rate of false detection, leading to bigger computational loads for the processor.

**Validation**

After processing the detected bursts, the estimated parameters for the three processors are passed to the validation algorithm. The validation algorithm has two main purposes: first, to remove outliers from the time series, and second, to select which of the three processor outputs will be used. The detection of outliers is performed by rejecting bursts which have a SNR below a certain threshold. The SNR for processor $k$, $SNR_k$, is calculated as:

$$SNR_k = \frac{\hat{P}_P^k}{\hat{P}_N^k C_a(\hat{f}_D^k)^2} \tag{27}$$

where $\hat{P}_P^k$ is the height of the power spectrum peak, $\hat{P}_N^k$ is the mean height of the noise level and $C_a(f)$ is a frequency dependent amplification factor that is necessary to compensate for imperfections in PMT and electronics used in the experiments. The experiment used to determine this factor is described in the section on the test experiments. In addition to the SNR, the probability of correct detection by the dual burst processors can be estimated. For the dual burst processor with temporal separation, the separation in time using the envelopes is the most crucial step: if the bursts cannot be correctly distinguished, the results are meaningless. The criterion

$$OCT_{ij} = \frac{\int_0^T \mathrm{ENV}_i(t)\,\mathrm{ENV}_j(t)\,dt}{\int_0^T (\mathrm{ENV}_j(t))^2\,dt} \approx \frac{\sqrt{2}A_2}{A_1}\frac{T_{t2}}{\sqrt{T_{t1}^2+T_{t2}^2}}e^{-\frac{8(T_{a1}-T_{a2})^2}{T_{t1}^2+T_{t2}^2}} \tag{28}$$

gives information about the impact of the overlap by burst $i$ on burst $j$. Tests with artificial bursts show that if $OCT_{ij}>0.15$ the location of burst j has probably been misdetected. Consequently, if $OCT_{12}>0.15$ or $OCT_{21}>0.15$ the burst pair is rejected. Similarly, the dual burst processor with spectral separation only produces useful results if the spectral peaks can be distinguished. If the spectral overlap criterion

$$OCF_{ij} = \frac{\int_0^{f_s/2} P_i(f)P_j(f)\,df}{\int_0^{f_s/2} (\mathrm{P}_j(f))^2\,df} \approx \frac{A_2^2T_{t2}^2}{A_1^2T_{t1}^2}\frac{\sqrt{2}}{\sqrt{T_{t1}^2+T_{t2}^2}}e^{-\frac{p^2T_{t1}^2T_{t2}^2(f_{d1}-f_{d2})^2}{4(T_{t1}^2+T_{t2}^2)}} \tag{29}$$

exceeds 0.1 for one of the two bursts the burst pair should be rejected since the spectral peak of burst j has likely been misdetected. If the smallest amplitude burst of a burst pair outputted by a dual burst processor is strongly clipped (it overlaps with the start or end of the signal block), the pair is also rejected. In addition, bursts corresponding to possible stray signals are rejected as well as burst pairs with strong temporal overlap (which originate from two particles present at the same time in the measurement volume). After these checks, the best processor estimate is selected from the remaining estimates: the processor estimate is chosen that has the smallest least squares norm:

$$L_k = \sum_{i=0}^{N-1} (s^k(t_i) - y(t_i))^2 \tag{30}$$

$L_k$ and $s^k(t)$ are the least squares norm and the model signal for processor k; y(t) is the input signal.

**6. TEST EXPERIMENTS**

Experiments to test the processor performance were performed in a laminar single phase flow and a bubbly flow. The LDA equipment consists of a 4W Spectra-Physics $Ar^+$ laser and a TSI 9201 colorburst multicolor beam separator. Beam pairs are focused using a backscatter probe. Detected light is sent to a TSI 9230 colorlink. For comparison purposes and setting of the equipment bursts are processed with processor type IFA-750 (TSI), controlled by a 486 PC. The electronic bandpass filtering is performed using the filters that are present in the IFA 750 equipment. Acquisition is performed using a dual channel fast ADC (Spectrum MI.3011) which is built in an Adlon 1700+PC with 4 striped harddisks with a total of 160 GB. This system allows for 8 or 12 bits acquisition of two channels at sampling frequencies up to 20 MHz each. Combined with the processing software, this provides a cheap (€5000 + costs of the PC) and powerful LDA processing unit.

Two flows were investigated. The first is a laminar pipeflow. A pipe (diameter 0.05 m) containing glycerol with viscosity around 35 mPas was used. The LDA setup used a 200 kHz preshift frequency and a backscatter probe with 0.25 m lens. The second flow is a bubbly flow. Air is injected into a rectangular container with dimensions 0.04 m x0.24 m x1.0 m (dxwxh), void fractions are in the range of 10% and bubble sizes around 4 mm. These experiments

had a 500 kHz preshift frequency, and an electronic bandpass range of 100-1000 kHz. The backscatter probe has a 0.122 m lens.
The frequency dependent amplification factor $C_a(f)$ (equation (27)) was determined using a sophisticated experiment where the signal amplitude was measured using a rotating disk. The Doppler frequency was varied by changing the velocity of the disk. Special care was taken to ensure a constant light intensity from the disk. The signal amplitude was found to vary up to a factor 2 within the specified range of the bandpass filters of the IFA-750 equipment. These filters were found to be a major cause of this problem. If no correction is performed severe biases in the velocity moments may result.

The single burst wavelet processor was tested using a laminar flow of glycerol in a pipe and results were compared with those from the IFA-750 processor (typical results shown in Table I). This showed that the wavelet technique gives a somewhat higher accuracy for the Doppler frequency at a much higher datarate. Of course, by increasing the SNR thresholds one can also reduce the datarate and measure with a higher accuracy. The IFA-750 data suffer from multiple validation: around 15% of the bursts are detected more than once. The wavelet processor shows negligible multiple validation.

**Table I. Results of test with laminar flow**

| | Datarate (Hz) | Multiple validation | $s_u/m_u$ |
|---|---|---|---|
| Wavelet Transform | 100 | Negligible | 5.3% |
| TSI IFA-750 | 35 | ≈15% | 6.8% |

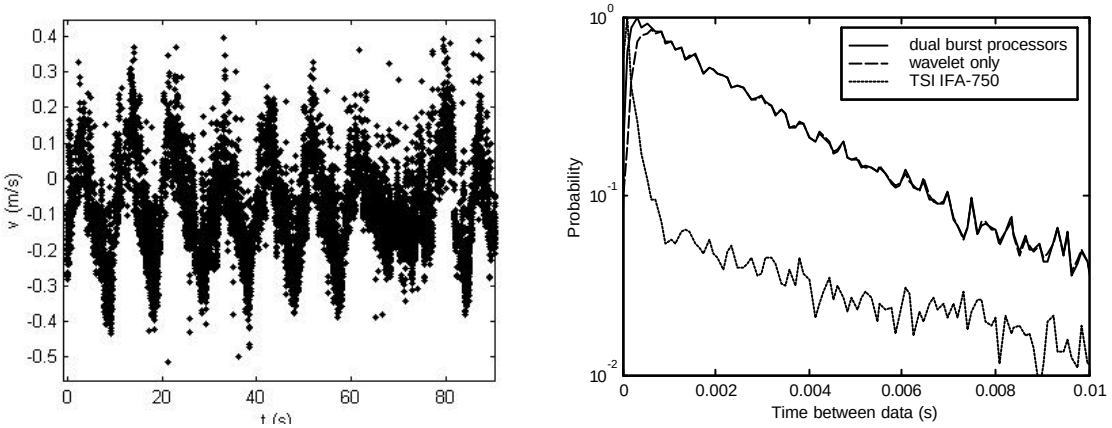


**Figure 12. a) Time signal for bubbly flow b) Particle interarrival time distribution**

The effect of the inclusion of the dual-burst processors is tested by using a bubbly flow: the more or less periodic liquid velocity in a flat bubble column is determined (Figure 12(a)). The presence of the bubbles leads to an increased amount of noise in the signal due to the light scattered by the bubbles. The use of the dual-burst wavelet processor increases the datarate again by a factor of 2-3 compared to the TSI IFA-750 output.
Figure 12(b) shows the distribution of the particle interarrival time. The random arrival of seeding particles should give a straight line on a log plot, with some curvature due to the presence of the bubbles for longer time intervals (longer than 5 ms). The graphs again show the multiple validation by the IFA-750 processor for short time intervals (<0.7 ms), and that this multiple validation is not present for the offline processors. Usage of only the wavelet technique gives a delay time of around 0.6 ms. Including the dual-burst processors reduces the delay time to around 0.3 ms, the average burst transit time. This shows that using the dual-burst processors we can estimate turbulence spectra up to higher frequencies and that the seeding density may be increased further.

The SNR threshold was set after inspection of the SNR of the estimated bursts versus the Doppler frequency (Figure 13). The figure reveals that many bursts are rejected. In addition, the bubbly flow is characterized by wide velocity pdfs. Therefore, the Doppler frequency, transit times etc. vary strongly. As a result, bias in the moments may occur with the current SNR definition (equation (27)). SNR definitions which suffer less from bias, however, make the datarate drop significantly since they provide less information about detectability. For these reasons, future studies will be aimed at investigation of other SNR definitions which reduce the bias but maintain reasonable datarates. In addition, the detector settings will be optimized to further reduce false detection to reduce the computational load.

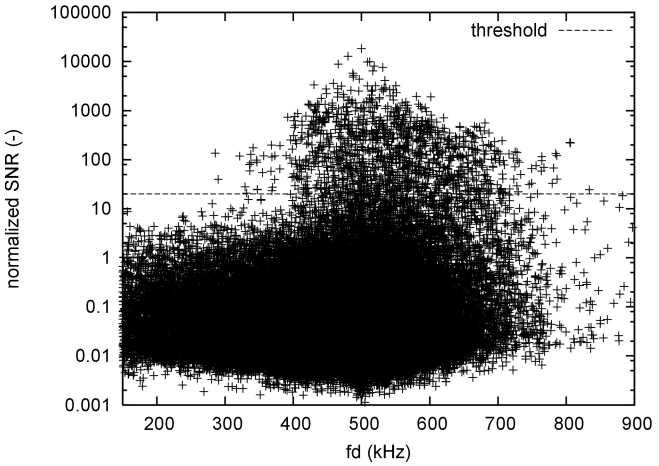


**Figure 13. SNR versus estimated Doppler frequency for bubbly flow**

## 7. CONCLUSIONS

The accurate measurement of turbulence spectra up to high frequencies requires data with high accuracy in both the Doppler frequency and the burst arrival time, as well as a short processor delay time, even in the presence of high noise levels. The procedure pursued in the present work is to limit the influence of noise and improve the accuracy of the Doppler frequency estimate and arrival time estimate by using the wavelet technique, i.e. a model of the burst is fitted to the data. The shorter delay time is achieved by allowing for dual bursts (i.e. overlapping bursts) by separating bursts either in the temporal or spectral domain. The direct use of the (iterative) wavelet technique for dual burst processing is limited by the peak broadening resulting in more difficult burst separation. Therefore, elements of the iterative wavelet technique were combined with separation techniques using the powerspectrum and envelope of the bandpassed signal, providing good results for both the burst separation and noise suppression. Tests show that the combination of the software burst detector, processor and validation routines allows increased datarates with similar accuracy if compared with a traditional commercial hardware processor. The particle interarrival time distribution shows that the processor delay time is effectively halved by the inclusion of the dual burst processors, allowing the investigation of turbulence spectra up to higher frequencies.

## ACKNOWLEDGEMENTS

The authors wish to thank Hans van Maanen and Holger Nobach for many useful discussions. Hans van Maanen is especially thanked for providing the initial algorithms on which parts of the software in this paper were based. In addition, Jaap Beekman is acknowledged for his work on the acquisition hardware and software.

## REFERENCES

Albrecht H.E., Borys M., Damaschke N. and Tropea C. (2003), "Laser Doppler and Phase Doppler Measurement Techniques", Springer-Verlag.

Benedict L.H., Nobach H. and Tropea C. (2000), "Estimation of turbulent velocity spectra from Laser Doppler data", Meas. Sci. Tech. 10, pp 138-145.

Broersen P.M.T., de Waele S. and Bos R. (2000) "The accuracy of time series analysis for laser doppler velocimetry", Proc. 10th Intl. Symp. On Appl. Of Laser Techniques to Fluid Mechanics, Lisbon, Portugal

Jenson L.M.T. (1992) "LDV digital signal processor based on autocorrelation", Proc. 8th Intl. Symp. On Appl. Of Laser Techniques to Fluid Mechanics, Lisbon, Portugal

Matovic D. and Tropea C. (1991) "Spectral peak interpolation with application to LDA signal processing", Meas. Sci. Techn. 2, pp 1100-1106.

Nobach, H. and Van Maanen, H.R.E. (2001) "LDA and PDA signal analysis using wavelets", Experiments in Fluids 30, pp 613-625.

Nobach, H. (2002) "Analysis of dual-burst laser Doppler signals", Meas. Sci. and Tech. 13, pp 33-44.

Van Maanen, H., Nijenboer, F.J. (1996), "Application of the wavelet transform to laser-Doppler processors", Proc. 8th Intl. Symp. On Appl. Of Laser Techniques to Fluid Mechanics, July, 8th-11th, Lisbon, Portugal

Van Maanen, H. (1999) "Retrieval of turbulence and turbulence properties from randomly sampled laser-Doppler Anemometry data with noise", Muiden, Netherlands.